Int. J. Heat Mass Transfer. Vol. 36, No. 15, pp. 3831–3839, 1993
Printed in Great Britain

0017–9310/93 $6.00 + 0.00

A sensitivity study of material properties for coupled convective–conductive heat transfer generated in an electronic equipment

H. Y. WANG and J. B. SAULNIER†
Laboratoire d'Etudes Thermiques, URA 1403 C.N.R.S., E.N.S.M.A., Poitiers, France

(*Received* 17 *September* 1991 *and in final form* 2 *February* 1993)

Abstract—The analysis of the conjugate heat transfer conduction/forced convection in a 2D channel constituted by two printed circuit boards (PCBs) with four uniformly heated integrated circuits (ICs) has been performed for steady-state conditions. The governing differential equations are solved in a primitive variables form, using a multigrid algorithm. The effects of the thermal conductivity of the materials constituting the PCBs and the ICs on the conjugate heat transfer have been studied through the evolution of the temperature and heat flux fields.

1. INTRODUCTION

IT IS WELL known today that the performances and the reliability of electronic chips are very sensitive to the junction temperature, and that the number of failures of circuits increases exponentially with this junction temperature. In order to satisfy the specific criteria for the chip temperature, each electronic equipment must be designed in such a way as to promote around it an efficient cooling. A sensitivity study of heat transfer can of course be performed on an experimental basis; the influences of some geometrical parameters, of power dissipation, have been reported in refs. [1, 2]. On the one hand, experimental studies are convenient because they clearly provide information that the numerical approach cannot, as yet, easily get, for example, the complexity of the 3D characteristics of the fluid flow itself. But on the other hand, they are quite time consuming, particularly for parametric studies, and they cannot offer as many details as the numerical results.

Therefore, numerical simulation is considered as a complementary means, which can be a very efficient tool in the case of parametric studies. Let us mention here some interesting numerical sensitivity studies of the heat dissipation [3], and of the geometry [4], for rather simple configurations (one or few ICs on the PCB), but very few contributions report the influence of the thermophysical parameters.

The present study concerns a steady-state and a laminar forced convection flow, and it investigates the sensitivity of heat transfer to the thermal conductivity of the materials in a particular electronic system composed of two printed circuit boards (PCBs) with four integrated circuits (ICs). Such a study provides a good understanding of the characteristics of the conjugate conduction/convection heat transfer between the air flow, the ICs (considered as dissipating blockages) and the PCBs. Also, the effect of changing the selected PCBs and ICs material is investigated to determine qualitative suggestions that might improve the thermal design of printed board assemblies. Let us mention that we are using a recent and powerful numerical procedure that we have adapted to the simulation of a 2D representation of this problem: the finite volume multigrid algorithm.

2. THE PROBLEM

Figure 1(a) shows the physical system to be simulated, which is an array of 20 heated rectangular epoxy or ceramic ICs mounted on one of the two boards constituting a channel. This configuration is chosen to simulate a typical electronic equipment currently encountered in the electronic industry. From the geometrical and thermophysical point of view, the ICs are practically identical and are settled row by row with a small spacing S_T between the rows. This particular 3D configuration will be transformed to allow an approximate simulation by a simplified two-dimensional model: a single row of ICs is modelled as illustrated in Fig. 1(b). It is clear that the width of the components L_T is less than the pitch of the array $(L_T + S_T)$ in the transverse direction z. However, to ensure correct heat input in the 2D analysis, the heat flux dissipated by each chip, which is considered as a very thin sheet without thickness, is calculated assuming a uniform heat flux in the transverse direction based on the pitch $(L_T + S_T)$ of the array (cf. Fig. 1(b)).

Finally, the physical system we keep in this two-dimensional analysis is an array of four heated ICs in

† *Correspondence to*: Professor J. B. Saulnier, E.N.S.M.A., Laboratoire d'Etudes Thermiques, rue Guillaume VII, 86034 Poitiers Cedex, France.

NOMENCLATURE

B	height of IC	S_L	streamwise spacing between the ICs
C_p	specific heat	S_T	transverse spacing between the ICs
e	plate thickness	T	temperature
G	grid level	T_e	inlet temperature
H	channel height	u	streamwise fluid velocity [m s^{-1}]
L	channel length	u_e	inlet velocity of streamwise fluid [m s^{-1}]
W	channel width	v	transverse fluid velocity [m s^{-1}]
L_L	streamwise dimension of an IC	x	streamwise coordinate
L_E	dimension of the inlet zone	y	transverse coordinate.
L_S	dimension of the outlet zone		
L_T	transverse dimension of an IC	Greek symbols	
L_C	chip length	λ	thermal conductivity [W m^{-1} K^{-1}]
NC	number of component	λ_f	thermal conductivity of the fluid [W m^{-1} K^{-1}]
P	prolongation operator	λ_s	thermal conductivity of the solid [W m^{-1} K^{-1}]
p	pressure	μ	dynamic viscosity [kg m^{-1} s^{-1}]
Q	heat dissipation of each IC [W]	ρ	volumetric mass [kg m^{-3}]
Q_{total}	total heat dissipation of the ICs [W]	ϕ	general variable.
q	volumetric flux density [W m^{-3}]		
R	restriction operator		

perfect contact with one wall of the channel, shown in Fig. 2. In general, a stack of such similar electronic boards is disposed side by side, as can be encountered, for instance, in telecommunication or computer racks. However, we have isolated two such boards (cf. Fig. 2) that we have supposed representative of a periodic thermal environment in this stack. One board supports the ICs, and other board delimits a channel in which the cooling air is flowing. The spacial periodicity in the y direction leads to what is called *thermal cyclic boundaries*. This means that the thermal condition which rules in the plan $y = 0$ is identical to that in the plan $y = H+e$.

Table 1 summarizes the geometrical dimensions defined in Figs. 1(a) and (b). In all the cases, the heat dissipation of each IC (Q = 1 W) is kept at the same value. Four different materials (starting from badly conductive, like epoxy, to fairly conductive, representative of a metallic core) for the PCBs, and two different materials (epoxy and ceramic which are practical important cases) for the ICs, have been chosen, and Table 2 summarizes their physical properties.

The inlet conditions are, respectively, u_e = 1.5 m s^{-1} for the velocity and T_e = 20°C for the tempera-

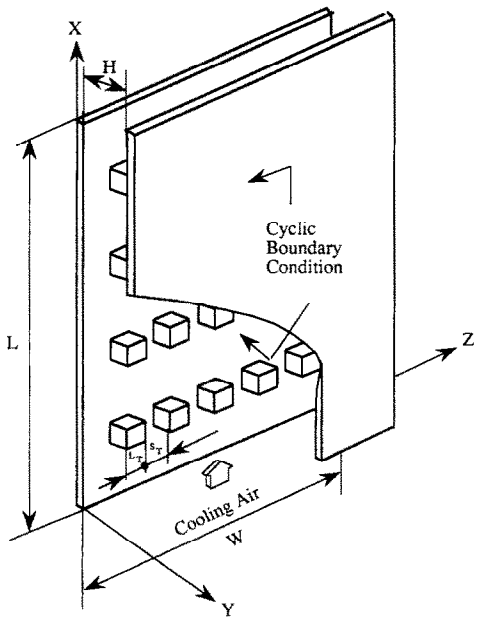

FIG. 1(a). The 3D electronic integrated circuits configuration.

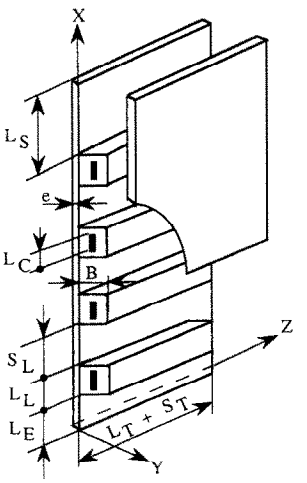

FIG. 1(b). The simplified 2D electronic ICs configuration.

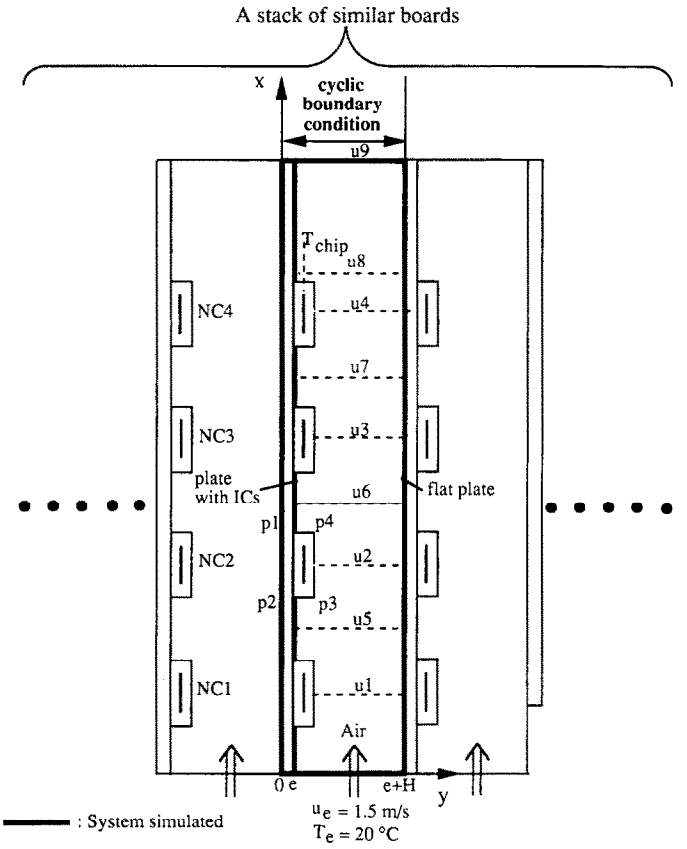

FIG. 2. The 2D model simulated.

ture. Let us also mention that in these conditions the flow is laminar ($Re = \rho u_e H/\mu$ is taken at about 1300) and that the problem is globally relevant of a steady-state analysis. The influence of the solid (PCBs and ICs) thermal conductivity we shall discuss is probably stronger in the present case of laminar regime; the heat transfer is less dominated by convective heat exchange as compared to what would happen for a turbulent regime.

Table 1. The geometrical dimensions and physical properties

Symbol	Value	Symbol		Value
L (mm)	170	L_C (mm)		15
H (mm)	15	B (mm)		5
L_E (mm)	15	e (mm)		2
L_S (mm)	50	q' (kW m^{-2})	NC1–4	4.44
L_L (mm)	15	λ_s (W m^{-1} K^{-1})	PCB	0.1–100
S_L (mm)	15		NC1–4	1–20
$L_T + S_T$ (mm)	15	λ_f (W m^{-1} K^{-1})		2.5×10^{-2}

3. GOVERNING EQUATIONS AND SOLUTION PROCEDURE

The flow considered here is governed by the steady, laminar incompressible Navier–Stokes equations in their fully elliptic form. The fluid properties are held constant for forced convection, the dynamic flow field is uncoupled from the temperature field, and the dynamic equations can be solved independently from the energy equation. These equations in Cartesian coordinates are

mass continuity

$$\frac{\partial u}{\partial x} + \frac{\partial v}{\partial y} = 0 \tag{1}$$

Table 2. The thermophysical properties of PCB and IC

ICs material	λ (W m^{-1} K^{-1})	Board material	λ (W m^{-1} K^{-1})	Board denomination
Case 1 (plastic type)	1	A (epoxy 1 type)	0.1	Badly conductive
		B (epoxy 2 type)	1.0	Less conductive
Case 2 (ceramic type)	20	C (ceramic type)	10.0	Good conductive
		D (metallic core type)	100.0	Fairly conductive

x-momentum

$$\rho u\frac{\partial u}{\partial x}+\rho v\frac{\partial u}{\partial y}=-\frac{\partial p}{\partial x}+\mu\frac{\partial^2 u}{\partial x^2}+\mu\frac{\partial^2 u}{\partial y^2} \quad (2)$$

y-momentum

$$\rho u\frac{\partial v}{\partial x}+\rho v\frac{\partial v}{\partial y}=-\frac{\partial p}{\partial y}+\mu\frac{\partial^2 y}{\partial x^2}+\mu\frac{\partial^2 v}{\partial y^2}. \quad (3)$$

A unique form is used to express the principle of energy conservation over the fluid and the solid regions.

$$\rho C_p u\frac{\partial T}{\partial x}+\rho C_p v\frac{\partial T}{\partial y}=\lambda\frac{\partial^2 T}{\partial x^2}+\lambda\frac{\partial^2 T}{\partial y^2}+q. \quad (4)$$

This equation holds over the entire computational domain, provided that the fluid velocity is set equal to zero in the solid region, which reduces the energy equation to pure conduction. As it is ultimately the control of temperature of the chips—located in the solid part (black layer in Fig. 2) and where the energy is dissipated—that is important, the coupling of the conduction in the packages and in the boards with the convection heat transfer in the fluid should be considered simultaneously. Such a conjugate conduction/convection heat transfer can be analyzed easily in laminar flow by using the harmonic averaging thermal conductivity at the interface between solid and fluid. Sometimes, this treatment gives rise to very strong anisotropies in the discretized coefficients and the problem has been effectively solved through the Block Correction Procedure [5].

The finite volume forms of the above differential equations are derived by integrating them over discrete control volumes [6] in the physical domain. A staggered mesh system is used in which the discrete velocities are located on the faces of the finite volume cells and the discrete pressures and temperatures are situated at the cells centres. The power-law scheme is used because it offers the best compromise between accuracy and stability.

For convenience in the use of the multigrid technique, the finite volume equations expressed per unit volume, can be written in the general form

$$a_P\phi_P-a_N\phi_N-a_S\phi_S-a_E\phi_E-a_W\phi_W=S_\phi\Delta x\Delta y \quad (5)$$

where ϕ stands for u, v, p and T, and S_ϕ is the source term in the appropriate direction. The coefficients a_P, $a_S\ldots$ and a_W represent the combined effects of convection and diffusion. The pressure–velocity linkage is resolved by a predictor–corrector technique, SIMPLEC [7].

To solve the set of the finite volume equations, we have to specify the boundary conditions, which can be expressed as follows:

at $x=0$ $\quad u=u_e \quad v=0 \quad T=T_e$

at $x=L$ $\quad \dfrac{\partial u}{\partial x}=\dfrac{\partial v}{\partial x}=\dfrac{\partial T}{\partial x}=0$

at $y=e$ and $y=H+e$

$u=v=0$ but T is unknown.

The planes at $y=0$ and $y=H+e$ are submitted to cyclic thermal boundary conditions ($T(x,0)=T(x,H+e)$) which have been handled, by using the cyclic tridiagonal matrix algorithm (CTDMA) [8].

4. MULTIGRID FOR NON-LINEAR PROBLEMS

The general concept of the multigrid technique [9] is well known, and will not be described here in detail.

It consists of a cyclic resolution of the model equations on a sequence of grids schematized as in Fig. 3 (fine G^3 and coarser ones G^2, G^1), which correspond together thanks to 'restriction' (R) and 'prolongation' (P) operators.

The procedure, called the smoother, we have retained to solve the model equations on a given level of grid, is the SIMPLEC algorithm, and as concerns the multigrid techniques, we have been operating with a FAS-FMG technique [10].

The restriction to the coarse grid velocities is defined as the arithmetic mean of two neighbouring nodes in the fine grid, whereas we use the four neighbouring nodes for scalar variables. The prolongation operator is derived in all cases by using bilinear interpolation. More details concerning the multigrid technique and its application can be found in [11].

5. RESULTS AND DISCUSSION

All the analyses presented here were performed using our computer code on a MicroVax (0.9 Mips), running under VMS. We had to define the optimum size of the finest grid for each case in order to obtain a solution independent of the grid, and as an example of performances, a $185(x)\times 105(y)$ grid on a sequence of four grid levels, for instance, needs about 55 min CPU.

Because the dynamic equations are independent of the conductivity of the materials, the velocity field is common to all the different cases, and we begin with some comments about the dynamic aspects. The adimensional u-velocity profiles across the channel for different positions defined in Fig. 2 are plotted in Figs. 4(a) and (b). The flow field starts with an imposed uniform velocity profile ($u/u_e=1$) at the channel inlet, and then varies much differently in the spanwise direction. The presence of the first blockage in the channel causes the flow to be diverted towards the smooth wall, resulting in an important distortion of velocity profile in the entrance region including the first IC referenced NC1 in Fig. 2. However, in the central blockages region (NC2, 3, 4), the profiles are rather periodic from one IC environment to another.

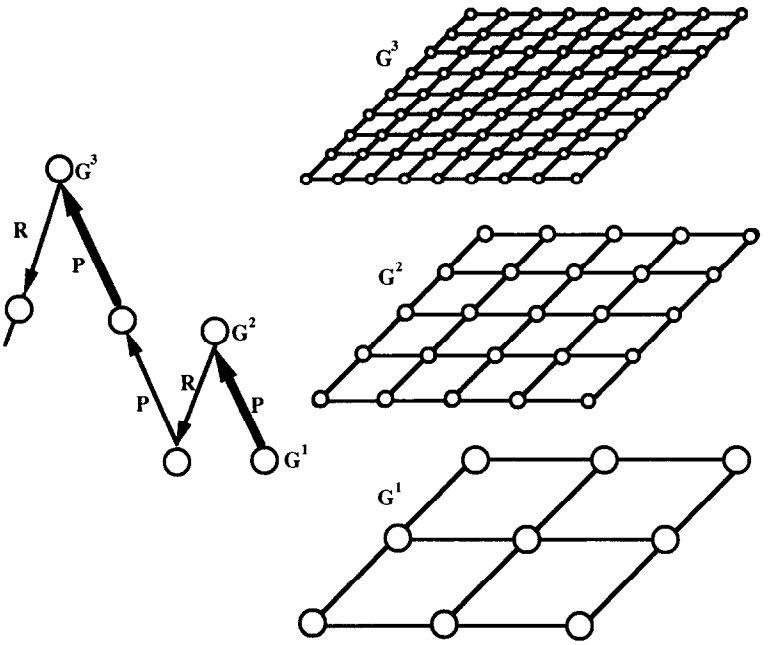

FIG. 3. Schematic of the multigrid strategy.

and the main flow concentrates in the central part of the gap between the channel and the components. Between the ICs, the velocity profiles also experience strong distortions due to the local variations of the cross-section along the channel, and the maximum velocity is shifted towards the smooth wall. Besides, a recirculating zone is clearly present behind each IC (curves 5, 6, 7), but the intensity of this recirculating flow is quite high across the section just downstream of the last blockage (curve 8). The distortion of the velocity profile (curve 9) in the exit is less remarkable; the blockages located upstream of here have less influence, and the maximum of the velocity has practically retrieved the central part of the channel, as in a smooth one.

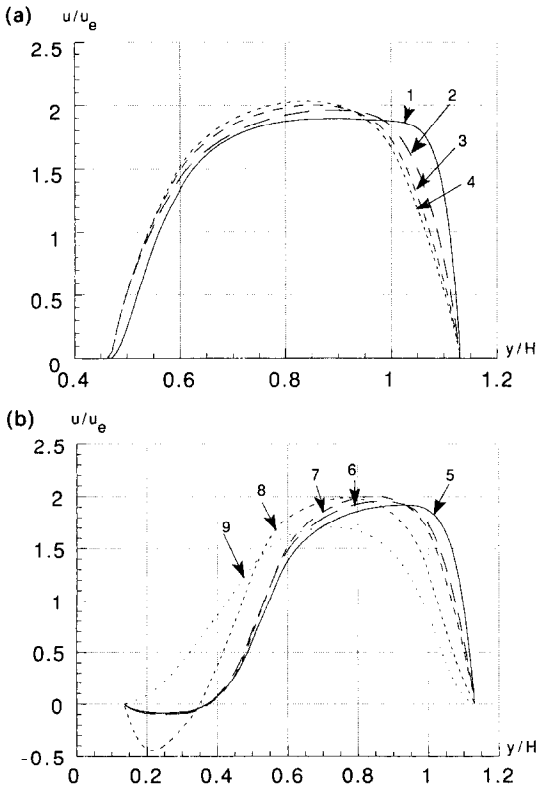

FIG. 4. Distribution of streamwise adimensional velocity.

We then separate the discussion of the results concerning the thermal aspect in two steps: the first one is relative to the case of epoxy ICs and the second to ceramic ICs. For each case, we discuss the influence of the conductivity of four different materials constituting the electronic board.

5.1. *Heat transfer sensitivity with epoxy-type integrated circuits*

We discuss here the influence of the board conductivity on the thermal field concerning the case of 'epoxy'-type ICs, which are themselves badly conductive ($\lambda = 1$ W m^{-1} K^{-1}) and will be combined with PCB of different conductivity (see Table 2 for the significance relative to cases A, B, C and D).

5.1.1. *Temperature distribution.* The temperature distribution along a streamwise line across the chip position is presented in Fig. 5, for which we comment as follows:

- the chip temperature increases rather regularly for the PCBs of small conductivity (cases A and B), when

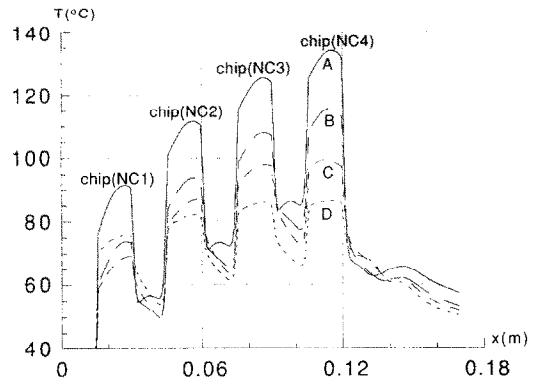

FIG. 5. Distribution of the chip temperature (epoxy IC).

progressing along the channel, from the component located in the inlet zone towards the outlet zone;

- in addition, a strong streamwise temperature gradient (up to 15°C) occurs even inside the IC for the case of badly conductive boards, and this gradient may induce, for instance, thermomechanical failures of the chip itself. This aspect remains, however, much less marked, in the cases C and D, where the PCBs are made with materials of good conductivity;
- the fact of using a fairly conductive PCB ($\lambda = 100$ W m^{-1} K^{-1}) causes a strong decrease of the chip temperature for the components NC2–NC4, precisely because of this fair conductivity of the board, the heat is collected by the board itself from the hottest components and is conducted to NC1, which, though located in the inlet region, is now at a higher temperature level; and
- finally, the presence of PCB made with materials of good conductivity reduces the increase of the chip's temperature along the channel, from the first component to the last one, and also decreases the temperature gradient inside the components.

5.1.2. *Heat flux distribution.* Let us first comment on the evolution of the flux convected to the air along the board surfaces and shown by Figs. 6(a) and (b). We observe that the thermal conductivity has an important influence on the flux convected along the plate with ICs (cf. Fig. 6(a)).

- For the badly conductive PCB (case A, $\lambda = 0.1$ W m^{-1} K^{-1}), the thermal exchanges in each interval between the components take place from the air (that has been heated by the components) towards the board, and the thermal flux becomes negative;
- for the less conductive PCB (case B, $\lambda = 1$ W m^{-1} K^{-1}), the exchanges in each interval between the components are still small, and they take place partly from the PCB board towards the air (positive flux) and, partly from the air towards the PCB (negative flux);
- as soon as one uses the good conductive PCB (cases C, $\lambda = 10$ or D, $\lambda = 100$ W m^{-1} K^{-1}), the air is always heated by the PCB in the interval between

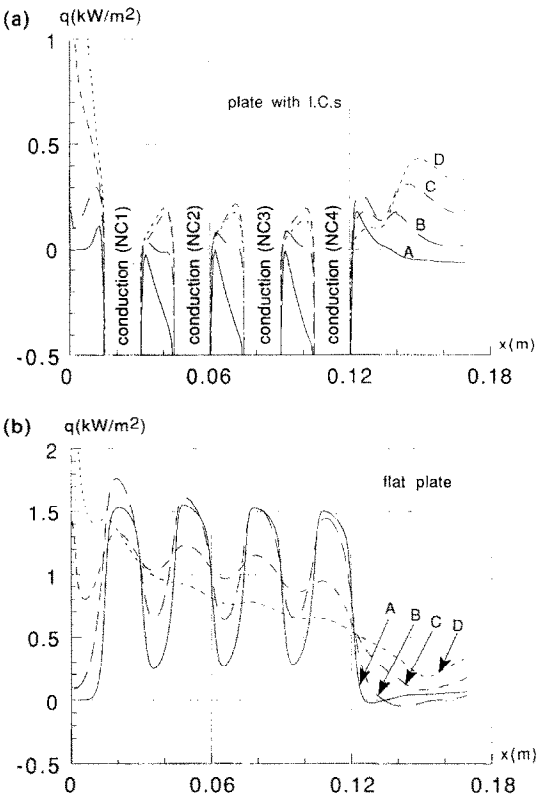

FIG. 6. Distribution of convected heat flux along the plates. (a) Plate with ICs; (b) flat plate.

the components and the convection has an effective cooling effect on this side of the board; and

- in the inlet and outlet zones, the convective flux is an increasing function of the PCB conductivity, and a negative flux appears in the outlet zone only for the badly conductive PCB ($\lambda = 0.1$ W m^{-1} K^{-1}).

The flux convected by the flat plate (that is without ICs) has a quite different evolution, and it is always of a higher order of magnitude (cf. Fig. 6(b)):

- the inlet zone is rather similar to what has been seen on the previous side; and
- the presence of the badly conductive PCB ($\lambda = 0.1$ or 1 W m^{-1} K^{-1}) leads to very important local perturbations of the convective flux, which may be very high in front of an IC, but becomes reduced up to 20% of its local maximum value in the zone between ICs. When the conductivity of the board increases, the flux distribution becomes smoother.

Figures 7(a) and (b) show the evolution of flux exchanged only around the components NC1 and NC2. In the study considered, the characteristics of the flux exchanged around the components NC3 and NC4 were found practically analogous to NC2. This figure also indicates some important dependence of the local effects on the board conductivity.

- On the surface 'p1p2' (see Fig. 2 for the contour definition) of the IC in contact with the PCB, the fact

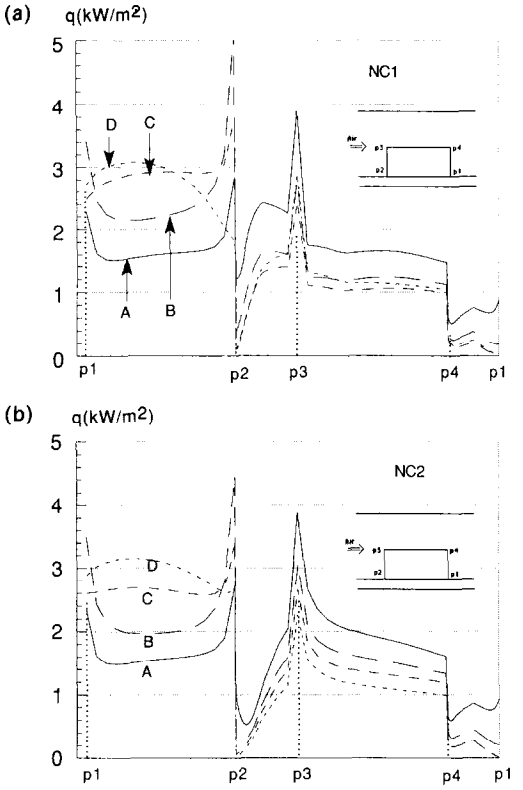

FIG. 7. Distribution of heat flux around the component. (a) Around the NC1; (b) around NC2.

of using a good or a fair conductive material for the board promotes more distinctly the conductive transfer towards the board for NC2, NC3 and NC4. However, the increased role of the conduction inside the fair conductive board drains more energy coming from the components NC2 and NC3. Consequently, at the level of the NC1, the global conductive transfer decreases and is partly compensated by a greater increase of the local convective transfer;

- in the case of a poorly conductive PCB, the convective transfer takes place more efficiently on the upstream surface 'p2p3' of the first component than on the corresponding surface of the others (NC2–4); this is likely due to the jet impingement effect on this first IC;
- on the surface 'p3p4' in contact with air, and if we exclude the first component (see previous comment relative to the conductive exchange through the surface 'p1p2'), the convective flux is a decreasing function of the PCB conductivity; and
- finally, on the surface facing downstream, 'p1p4', the presence of the badly conductive PCB clearly induces a relatively higher value of the convective flux.

Table 3 summarizes for all four materials the distribution of the flux convected by the flat plate, by the plate with ICs, and by the different surfaces of the ICs which are themselves in contact with air. As a summary of this sensitivity of the local heat transfer to the conductivity of the board material, we can observe that:

- an increase of the PCB conductivity reduces the flux directly convected around the components and makes better use of the part of the board with or without the ICs, which becomes a more efficient fin; and
- the board itself drains more and more heat flux coming from the downstream components towards the inlet zone where it is carried away by the cold inlet fluid, thanks to an efficient thermal exchange. Besides, for fairly conductive material, this flux longitudinally conducted through the board reduces the conduction from NC1 to the board and induces a temperature slightly higher for this first IC.

5.2. *Heat transfer sensitivity with ceramic type integrated circuits*

We consider here the case where the ICs are made of ceramic, but still combined with the same four PCB materials. But we discuss two IC configurations which only differ by the presence or absence of a cavity filled with nitrogen inside the ICs. In each case, the geometry here is identical to the epoxy ICs configuration, and the contact with the board is a perfect one. The IC conductivity of the first configuration is still uniform with the value of 20 $W\,m^{-1}\,K^{-1}$, whereas the second configuration is heterogeneous, and is composed partly by ceramic ($\lambda = 20$ $W\,m^{-1}\,K^{-1}$) and partly by nitrogen ($\lambda = 0.035$ $W\,m^{-1}\,K^{-1}$). The presence of the nitrogen cavity is currently encountered in usual ceramic ICs and its structure is a bit more complex, as shown in Fig. 8. The results we present for the second configuration correspond to another grid size $217(x) \times 105(y)$ which was found as the optimal finest grid on a sequence of four grid levels.

Table 3. Flux distribution around the ICs and along the PCBs

Flux / PCB type	Convected flux (Q_{total} (%))		
	Flat plate	Plate with ICs	All around the ICs (%)
A (epoxy 1 type)	42.35	−3.95 (air heats the board)	61.6
B (epoxy 2 type)	49.75	3.75	46.5
C (ceramic type)	50.85	11.27	37.88
D (metallic core type)	49.6	17.6	32.8

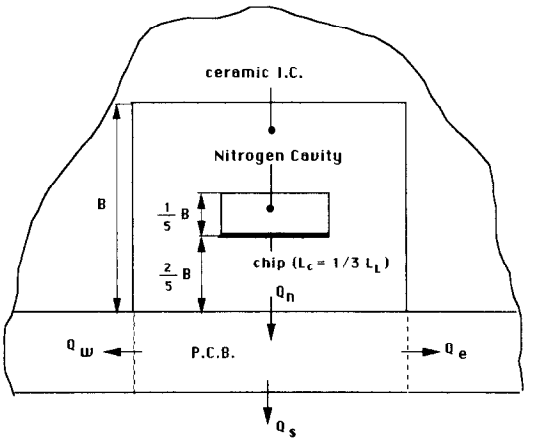

FIG. 8. The internal structure of the ceramic component.

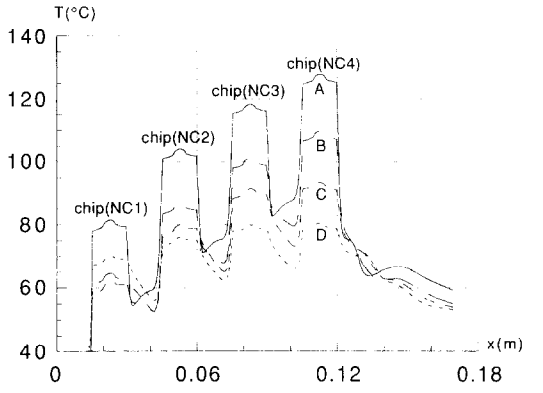

FIG. 10. Distribution of the chip temperature (ceramic IC with nitrogen cavity).

The temperature distributions along the line across the chip position were compared for the full ceramic IC and for the ceramic IC with the presence of the nitrogen cavity. Figures 9 and 10 show that the chip temperature behaviour for the two types of ceramic IC is rather analogous to what we have already observed in the case of epoxy ICs (cf. Fig. 5). However, the presence of full ceramic ICs induces a decrease of the highest temperature value (between 5 and 10°C), and the strong temperature gradient now disappears inside the ICs, whatever the thermal conductivity of the PCBs may be. We observe also that the presence of the nitrogen cavity inside the ceramic IC leads to only a small and local temperature increase of 3°C, and a relatively stronger gradient at the chip level as compared to that of full ceramic IC.

In short, for the three cases we have studied here, the type of IC perfectly attached on the board results in small effects on the maximum chip temperature, and the properties of the board seem to be the main governing parameter. When replacing the full epoxy case by a full ceramic one, the maximum temperature level on the chip decreases by about 5°C. Besides, the great streamwise gradient encountered in the epoxy

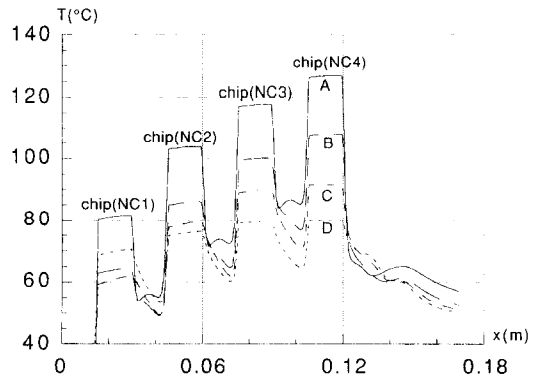

FIG. 9. Distribution of the chip temperature (full ceramic IC).

IC is suppressed when using ceramic IC. The introduction of a nitrogen cavity in the ceramic case (with the same global geometry and power dissipation, but a slightly different power distribution) only leads to a slight and local increase of the chip temperature. It is likely that in the case of imperfect contact between the IC and the board, the properties of IC would then become the prevailing parameters.

6. CONCLUSION

Thanks to the efficient numerical multigrid technique we especially adapted to the context of electronic PCBs, we could perform a sensitivity study of the temperature and flux fields to different constitutive materials. The procedure has been demonstrated to be computationally very efficient, even in the case of high anisotropies in the thermal diffusion coefficients, and allows cyclic thermal boundary conditions to be easily accommodated.

The detailed analysis of the thermal flux for the epoxy case clearly indicated that the effect of coupling of convection with conduction in the solids can strongly affect the thermal behaviour of electronic ICs, making the temperature and heat flux distributions very difficult to predict by conventional analytical methods.

The second and third cases (full ceramic IC or IC with nitrogen cavity) showed that the heat exchanges are less sensitive to the component materials than to the PCB ones, whatever the component structure may be, because in all the configurations we assumed a perfect contact between the ICs and the board.

As a general conclusion, in all cases it also becomes evident that the increase of the PCB conductivity promotes the enhancement of the conductive flux from the downstream hotter components towards the inlet zone where the convective exchanges are distinctly more efficient. Consequently, the conjugated effects contribute, on the one hand, to decrease the highest chip temperature value, and on the other hand, to induce a slightly higher chip temperature value for the first component.

REFERENCES

1. R. J. Moffat, D. E. Arvizu and A. Orgeta, Cooling electronic components: forced convection experiments with an air-cooled array, *Heat Transfer In Electronic Equipment* HTD-Vol. 48, 17–27 (1985).
2. A. Ortega and R. J. Moffat, Buoyancy induced convection in a non-uniformly heated array of cubical elements on a vertical channel wall, *Heat Transfer In Electronic Equipment* HTD-Vol. 57, 123–134 (1986).
3. M. Afrid and A. Zebib, Natural convection air cooling of heated components mounted on a vertical wall, *Numer. Heat Transfer, Part A* **15,** 243–259 (1989).
4. S. Habchi and S. Acharya, Laminar mixed convection in a partially blocked, vertical channel, *Int. J. Heat Mass Transfer* **29,** 1711–1722 (1986).
5. A. Settari and K. Aziz, A generalization of the additive correction methods for the iterative solution of matrix equations, *SIAM J. Numer. Anal.* **10,** 506–521 (1973).
6. S. V. Patankar, *Numerical Heat Transfer and Fluid Flow*. McGraw-Hill, New York (1980).
7. J. P. Van Doormaal and G. D. Rathby, Enhancements of the SIMPLE method for predicting incompressible fluid flow, *Numer. Heat Transfer* **7,** 147–163 (1984).
8. S. V. Patankar, C. H. Liu and E. M. Sparrow, Full developed flow and heat transfer in ducts having streamwise-periodic variations of cross-sectional area, *Trans. ASME, Ser. C, J. Heat Transfer* **99,** 180–186 (1977).
9. A. Brandt, Multi-level adaptive solution to boundary-value problems, *Mathematics of Computation* **31**(138), 333–390 (1977).
10. S. P. Vanka, Block-implicit multigrid solution of Navier–Stokes equations in primitive variables, *J. Comput. Phys.* **65,** 138–158 (1986).
11. H. Y. Wang, Simulation Numérique par Multigrilles des Transferts Conjugués dans les Cartes de Composants Electroniques, Thèse No. d'ordre: 405, Université de Poitiers (1991).